HHS Public Access

Author manuscript

Nat Neurosci. Author manuscript; available in PMC 2020 October 28.

Published in final edited form as:

Nat Neurosci. 2019 June ; 22(6): 933–940. doi:10.1038/s41593-019-0389-0.

Memory formation in the absence of experience

Gisella Vetere[1,10], **Lina M. Tran**[1,2], **Sara Moberg**[1], **Patrick E. Steadman**[1,3], **Leonardo Restivo**[1], **Filomene G. Morrison**[4,5], **Kerry J. Ressler**[6], **Sheena A. Josselyn**[1,2,3,7,8,*], **Paul W. Frankland**[1,2,3,7,9,*]

[1]Program in Neurosciences and Mental Health, Hospital for Sick Children, Toronto, Ontario, Canada.

[2]Department of Physiology, University of Toronto, Toronto, Ontario, Canada.

[3]Institute of Medical Sciences, University of Toronto, Toronto, Ontario, Canada.

[4]National Center for PTSD at VA Boston Healthcare System, Boston, MA, USA.

[5]Department of Psychiatry, Boston University School of Medicine, Boston, MA, USA.

[6]McLean Hospital, Harvard Medical School, Belmont, MA, USA.

[7]Department of Psychology, University of Toronto, Toronto, Ontario, Canada.

[8]Brain, Mind and Consciousness Program, Canadian Institute for Advanced Research, Toronto, Ontario, Canada.

[9]Child and Brain Development Program, Canadian Institute for Advanced Research, Toronto, Ontario, Canada.

[10]Present address: Laboratoire Plasticité du Cerveau, ESPCI- École Supérieure de Physique et de Chimie Industrielles, Paris, France.

Abstract

Memory is coded by patterns of neural activity in distinct circuits. Therefore, it should be possible to reverse engineer a memory by artificially creating these patterns of activity in the absence of a sensory experience. In olfactory conditioning, an odor conditioned stimulus (CS) is paired with an unconditioned stimulus (US; for example, a footshock), and the resulting CS–US association guides future behavior. Here we replaced the odor CS with optogenetic stimulation of a specific olfactory glomerulus and the US with optogenetic stimulation of distinct inputs into the ventral tegmental area that mediate either aversion or reward. In doing so, we created a fully artificial

[*]**Correspondence and requests for materials** should be addressed to S.A.J. or P.W.F. sheena.josselyn@sickkids.ca; paul.frankland@sickkids.ca.

Author contributions

G.V. and P.W.F. conceived the study and designed the experiments. G.V., L.M.T., and S.M. conducted the behavioral and immunohistochemical experiments. G.V. and L.R. conducted data and statistical analyses. P.E.S. conducted the iDISCO tissue clearing. P.W.F., G.V., K.J.R., F.G.M., and S.A.J. wrote the paper.

competing interests

The authors declare no competing interests.

Additional information

Supplementary information is available for this paper at https://doi.org/10.1038/s41593-019-0389-0.

Reprints and permissions information is available at www.nature.com/reprints.

memory in mice. Similarly to a natural memory, this artificial memory depended on CS–US contingency during training, and the conditioned response was specific to the CS and reflected the US valence. Moreover, both real and implanted memories engaged overlapping brain circuits and depended on basolateral amygdala activity for expression.

Animals readily learn to associate cues present in the environment with biologically salient events; for example, the presence of an appetitive food stimulus or aversive danger stimulus. Memory for this association then guides future decisions, promoting approach or avoidance, respectively, of these previously neutral environmental cues. Classical approaches, as well as more recent molecular and transgenic approaches, have localized key components of memory traces underlying these types of associations to specific brain regions and neural circuits. In parallel, electrophysiological and imaging approaches have identified patterns of neuronal activity that correspond to particular experiences[1–3]. Therefore, given this current level of understanding about how memories are localized and coded in the brain, it should be possible to reverse engineer this process and artificially implant a memory for an otherwise never experienced event.

To successfully implant an artificial memory, two criteria have been proposed[4]. First, the ‘learning event’ should take place entirely intracranially, which can be via, for example, direct stimulation of the brain. Second, the presence of the implanted memory should be demonstrated via the presentation of a ‘real’ external sensory retrieval cue. The behavioral manifestation of this memory retrieval should accurately reflect the predicted content of the stored information (in the example above, approach for an appetitive stimulus or avoidance for an aversive stimulus). Moreover, behavioral responding (reflecting memory retrieval) should be restricted to the ‘trained’ cue (and not unrelated cues).

In the laboratory, conditioning has typically been studied using tones, lights, or contexts as initially neutral sensory cues. While these more complex stimuli act as effective CS events in a range of paradigms, it is difficult to predict which patterns of neural activity correspond to a specific stimulus a priori. Consequently, they are difficult to recreate artificially via direct stimulation of the brain. In contrast, the anatomical and molecular organization of the olfactory system is well characterized in the mouse and spatially stereotyped across individuals[5–10]. Here, these properties allowed us to mimic an external odor CS via direct stimulation of a specific olfactory glomerulus. We paired this olfactory glomerulus stimulation with either rewarding or aversive artificial brain stimulation (the US). We then determined whether these intracranial conditioning procedures had resulted in memory implantation by presenting an external, retrieval cue (odor) that the mouse had not previously experienced. We found that presentation of an odor (acetophenone) that corresponded to the targeted olfactory glomerulus (and, importantly, not another odor) induced natural memory recall. That is, the mice either approached or avoided this odor depending on the valence (positive or negative, respectively) of the US pathway we stimulated during training.

Results

Pairing acetophenone with footshock produces conditioned odor aversion.

We first trained mice to form a real odor associative memory[11,12]. During training, an odor CS, acetophenone, was paired with delivery of a mild footshock US. Memory was assessed 1 day later in a neutral, novel, rectangular apparatus containing the conditioned odor (acetophenone) and a distinct odor (carvone) at either end (Fig. 1a; Supplementary Fig. 1). Notably, acetophenone and carvone activate distinct odorant receptor (OR) populations.

During this memory test, conditioned mice avoided the acetophenone odor, spending more time on the carvone side of the apparatus. Training-naive mice did not show a preference for either side of the apparatus, indicating that there was no innate aversion or attraction to either odor. Moreover, conditioning depended on the pairing of the CS and US during training. Mice presented with the CS and the US in a temporally unpaired manner during training (US | CS group) or the CS or US alone (CS only, US only groups) did not avoid the CS (acetophenone) in subsequent tests (Fig. 1b,c). Preference was not confounded by the distance traveled by the mice in the test session (Supplementary Fig. 2).

Pairing M72 photostimulation with footshock produces conditioned odor aversion to the M72-activating odorant acetophenone.

In the nose, odors are detected by olfactory sensory neurons (OSNs), which are dispersed across the olfactory epithelium. In mice, each OSN expresses one of ~1,000 distinct types of ORs, and axons from OSNs expressing the same OR converge onto one or two glomeruli in each olfactory bulb[5–10]. Acetophenone, but not carvone, strongly activates OSNs expressing the M72 OR (encoded by the *Olfr160* gene[13]) (Supplementary Fig. 3).

This stereotyped anatomical and molecular organization of the olfactory system makes it possible to genetically target specific OSNs in the mouse. Therefore, we next tested whether it is possible to replace the presentation of acetophenone (an M72-activating odorant, real CS) with direct optogenetic stimulation of the M72 olfactory glomerulus (and therefore the associated M72-expressing OSN axon terminals, artificial CS) in our conditioning paradigm. We used mice that express a channelrhodopsin 2–yellow fluorescent protein (YFP) fusion protein in M72-expressing OSNs (M72-ChR2 mice)[14] (Fig. 1d,e; Supplementary Video). During training, photostimulation of the M72 glomerulus (10 s, 4 Hz) was paired with footshock delivery (1 s, 0.7 mA) for 10 trials. (Supplementary Fig. 4). Although these mice had never previously been exposed to acetophenone, they avoided this M72-activating odorant during the subsequent test, spending more time on the carvone side of the apparatus. Similar to conditioning with an actual odor, learning produced by optogenetic stimulation of M72 depended on the pairing of the artificial CS and footshock US during training. Mice that received either M72 photostimulation alone (CS only group) or mice in which M72 photostimulation and footshock delivery was unpaired during training (US | CS group) exhibited no preference (Fig. 1f,g). These controls indicate that photostimulation of the M72 glomerulus does not alter the preference of the mice to the M72-activating odor acetophenone.

Pairing M72 photostimulation with photostimulation of LHb inputs to the VTA produces conditioned odor aversion to the M72-activating odorant acetophenone.

In these experiments, trained mice avoided acetophenone even though they had not encountered this odor before. However, there remains an experiential, somatosensory component to the learning since footshocks were delivered during training. Therefore, we next tested whether memory formation was possible in the absence of experience by additionally replacing the aversive US with direct optogenetic stimulation. A previous study[15] identified a projection from the lateral habenula (LHb) to the medial ventral tegmental nucleus (VTA) that mediates aversion. Therefore, we reasoned that direct stimulation of this pathway might mimic an aversive US. To optogenetically target this pathway, we injected an adeno-associated virus expressing channelrhodopsin 2 (AAV-ChR2) into the LHb, and implanted an optrode above the labeled terminal projections in the medial VTA in M72-ChR2 mice (Fig. 2a–c). During training, we paired photostimulation of the M72 glomerulus (CS) with photostimulation of LHb–medial VTA projections (US) (Supplementary Fig. 5), and then tested the preference for real odors 1 day later. In this test, mice avoided the acetophenone (M72-activating odorant) side of the apparatus. Similar to mice conditioned with real stimuli, this avoidance depended on the pairing of the artificial CS and artificial US, since avoidance was not observed in the unpaired training condition (US | CS group) (Fig. 2d,e).

Pairing M72 photostimulation with photostimulation of LDT inputs to the VTA produces conditioned odor attraction to the M72-activating odorant acetophenone.

A second input from the laterodorsal tegmental nucleus (LDT) to the lateral VTA mediates rewarding signals[15], and pairing acetophenone with a food reward induces preference for the acetophenone side of the apparatus (Supplementary Fig. 6). Therefore, we next determined whether pairing photostimulation of the M72 glomerulus with photostimulation of this rewarding pathway would induce attraction, rather than aversion, to M72-activating odorants such as acetophenone. We microinjected AAV-ChR2 into the LDT and implanted an optrode above labeled terminal projections in the lateral VTA in M72-ChR2 mice (Fig. 2f–h). During training, we paired photostimulation of the M72 glomerulus (CS) with photostimulation of reward-inducing LDT–lateral VTA projections (US) (Supplementary Fig. 5), and then tested the preference for real odors 1 day later. In this test, mice spent more time in the acetophenone side of the apparatus. Similar to the avoidance memory, this conditioned attraction depended on pairing the artificial CS with the artificial US during training (that is, no preference was exhibited in the US | CS group; Fig. 2i,j).

The absence of odor preference in this unpaired condition again supports the idea that there is no innate aversion or attraction for either of the two test odorants. More importantly, our finding that VTA photostimulation supported either conditioned aversion or attraction depending on which input pathway was targeted excludes the possibility that nonspecific heat or light effects of VTA photostimulation act as an aversive US in these experiments. Consistent with this, pairing acetophenone with VTA photostimulation (in the absence of ChR2 expression) did not produce conditioned aversion of acetophenone (Supplementary Fig. 7).

Retrieval of artificial and real odor memories engages similar neural circuits.

In these experiments, mice behaved as if they had experienced a specific past sensory event. Therefore, we next tested whether this artificial memory and the real odor memory engaged similar neural circuitry. Mice were randomly assigned to one of the two following training conditions: CS only (that is, acetophenone or M72 photostimulation) or CS + US (that is, acetophenone + shock or M72 photostimulation + LHb–medial VTA aversive photostimulation) (Fig. 3a,b). Following training, induction of the activity-regulated gene *Fos* was assessed in 18 brain regions, including central olfactory system regions and regions implicated in associative memory (Fig. 3c). Post-training CS presentation (that is, acetophenone or M72 photostimulation) induced widespread c-Fos expression within these regions in both CS only and CS + US groups compared with naive (home cage) controls (Fig. 3d,e; Supplementary Fig. 8). Notably, across brain regions, levels of c-Fos expression were highly correlated between both real and artificial conditions (CS only: $r = 0.80$, $P < 0.001$; CS + US: $r = 0.77$, $P < 0.005$; Supplementary Fig. 9), suggesting that acetophenone presentation and M72 photostimulation activated similar neural circuits. However, learning-specific activation (that is, CS + US > CS only) was observed only in the basolateral amygdala (BLA) for both real and artificial memories (Fig. 3f–i).

The BLA is essential for recall of artificial and real odor memories.

The above analysis suggested that the BLA is a region where CS and US signals might interact during artificial conditioning. Previous studies have indicated that this region plays a key role in real odor fear memories[16]. Therefore, we next tested whether chemogenetic silencing of the BLA before testing would similarly block expression of artificially generated odor memories. We virally expressed the inhibitory DREADD (designer receptor exclusively activated by designer drug) hM4Di in the BLA, and then injected the DREADD agonist 21 (C21)[17] or vehicle before testing.

For the real memory group, wild-type (WT) mice received acetophenone paired with footshock during training (Fig. 4a–c). In a preference test 1 day later, vehicle-treated mice avoided the acetophenone side of the apparatus. In contrast, mice treated with C21 before testing expressed no preference (Fig. 4d,e). We additionally trained groups of mice that did not express hM4Di in the amygdala, and injected them with either vehicle or C21 before testing. In this preference test, both vehicle-treated and C21-treated mice avoided the acetophenone side of the apparatus (Supplementary Fig. 10). This result indicates that impaired memory expression requires both the receptor (hM4Di) and ligand (C21), and excludes the possibility that C21 alone is responsible for altered behavior.

For the artificial memory group, M72-ChR2 mice received photostimulation of the M72 glomerulus paired with photostimulation of the aversion-inducing LHb–medial VTA projection (Fig. 4f–h). In a preference test 1 day later, vehicle-treated mice avoided the acetophenone side of the apparatus, whereas C21-treated mice expressed no preference (Fig. 4i,j). In a subset of mice, we confirmed that C21 treatment reduced the activation of hM4Di-expressing neurons in the BLA following recall of real and artificial memories (Supplementary Fig. 11). These results confirm previous inactivation studies showing that the BLA plays an essential role in the expression of olfactory fear memories[16,18]. The results

also reveal a similarly essential role for BLA activity in the expression of artificially generated odor fear memories.

Discussion

Previous engram studies in mice have tagged neuronal populations that are active during learning with excitatory and inhibitory opsins[2,3]. Subsequent manipulation of these experience-tagged neuronal populations may invoke memory expression in the absence of retrieval cues[19–22], prevent memory expression in the presence of retrieval cues[20,23–25], or allow experienced stimuli to become associated with new stimuli[26,27] or with one another[25,28]. In contrast, in the current study, memory formation occurred in the absence of any sensory experience (either CS or US). The resulting artificial memory shared many characteristics with a real odor memory. Its formation depended on CS and US contingency during training. Moreover, both real and artificial memories engaged similar neural circuits and depended on BLA activity for their expression. Although memory may be characterized as the retention of experience-created (or modified) representations across time[29], the current study indicates that it is possible to entirely bypass experience and, via direct stimulation of the brain, implant a specific memory in mice.

Our study builds on notable earlier work that used electrical stimulation to target brainstem and cerebellar circuits controlling conditioned motor reflexes in awake, behaving rabbits[30,31]. In these experiments, putative CS and US pathways were stimulated. Following paired stimulation of these pathways, direct stimulation of the CS pathway alone was sufficient to produce conditioned responding. Since conditioning was accomplished via direct electrical stimulation of the brain, these studies address the first criterion suggested for memory implantation. That is, ‘learning’ should be accomplished entirely intracranially[4].

However, these earlier studies did not address the second criterion. That is, demonstration of memory implantation via presentation of a real external sensory retrieval cue[4]. In the earlier work with rabbits[30,31], the conditioning procedure did not lead to the implantation of any specific information in the brain. Rather, paired direct stimulation induced some plasticity in the cerebellum, which could then be read out via stimulation of the same circuit[30,31]. In contrast, in the current work, the precise anatomical and molecular organization of the olfactory system allowed us to mimic an external odor CS via direct stimulation of a specific olfactory glomerulus. This allowed us to test whether our intracranial conditioning procedures had resulted in memory implantation by presenting an external retrieval cue (odor) that the mouse had not previously experienced. We found that presentation of an odor (acetophenone) that corresponded to the targeted olfactory glomerulus (and, importantly, not another odor) induced natural memory recall. That is, the mice either approached or avoided this odor depending on the valence (positive or negative, respectively) of the US pathway we stimulated during training.

While our intracranial stimulation procedures induced artificial conditioning, several questions remain. First, how do artificial CS and US signals interact in the brain? We found that BLA activity was necessary for the expression of both real and artificial odor memories. This finding is consistent with previous studies showing that plasticity in this region plays a

key role in the formation and expression of odor fear memories[18,32,33]. Therefore, the BLA represents at least one point of convergence between CS and US signals during this type of conditioning. However, this does not exclude the possibility that CS and US signals interact elsewhere in the brain during real and artificial odor conditioning. Indeed, during real odor conditioning, plastic changes may even occur in OSNs in the nose and in their synapses in the olfactory bulb, indicating convergence may additionally occur at very early stages of sensory processing[11,12,34].

Second, might photostimulation of other putative US pathways additionally support conditioning? In our experiments, we targeted inputs to the VTA. The advantage of targeting this region was that equivalent VTA photostimulation could be used to condition either attraction or aversion depending on which input was targeted[15]. However, these pathways do not represent the only pathways that can provide instructive signals during conditioning[35]. For example, activation of the periaqueductal gray[36–38], the parabrachial nucleus[39,40], and the anterior cingulate cortex[41,42] may support aversive learning. Similarly, activation of mesolimbic circuits may support appetitive learning[43]. It is likely that combining M72 photostimulation with photostimulation of these regions or pathways would similarly induce conditioned avoidance and attraction, respectively.

online content

Any methods, additional references, Nature Research reporting summaries, source data, extended data, supplementary information, acknowledgements, peer review information; details of author contributions and competing interests; and statements of data and code availability are available at https://doi.org/10.1038/s41593-019-0389-0.

Methods

Mice.

Two lines of mice were used in these experiments. We used WT mice in experiments in which acetophenone was paired with either footshock or food to produce real odor memories. These WT mice were F1 progeny derived from a cross between C57BL/6NTac and 129S6/SvEvTac mice (Taconic Farms). In experiments in which photostimulation of the M72 olfactory glomerulus was paired with footshock or stimulation of inputs into the VTA, we used transgenic M72-ChR2 mice[14]. These mice were obtained from the Jackson Laboratory on a mixed C57B6/129 background (stock number 021206). Experimental transgenic mice were the F1 offspring produced by breeding homozygous M72-ChR2 mice.

All mice were bred in our colony at The Hospital for Sick Children. After weaning at postnatal day 21, same sex mice were group-housed in standard mouse housing cages (2–5 per cage). Rooms were maintained on a 12 h light–dark cycle, and behavioral testing occurred during the light phase of the cycle. Mice were 8–9 weeks of age at the start of all experiments. Both male and female mice were used in all experiments, and mice were randomly assigned to different experimental conditions. All procedures were approved by The Hospital for Sick Children Animal Care and Use Committee and conducted in

accordance with the Canadian Council on Animal Care and the US National Institutes of Health guidelines on the Care and Use of Laboratory Animals.

Surgery.

Anesthesia.—Mice were pretreated with atropine sulfate (0.1 mg per kg, intraperitoneally (i.p.)), anesthetized with chloral hydrate (400 mg per kg, i.p.), and then placed into stereotaxic frames. After surgery, mice were treated with analgesic (Ketoprofen, 5 mg per kg, subcutaneously) and 1 ml of 0.9% saline (subcutaneously) to prevent dehydration

Virus infusion.—Viral vectors were microinjected (1.2 μl per side at a rate of 0.1 μl min^{-1}) into the target region via glass micropipettes connected via polyethylene tubing to a microsyringe (Hamilton). Micropipettes remained in place for 5 min after microinjection to ensure virus diffusion. To target projections to the VTA with an excitatory opsin, AAV5-CaMKIIa-hChR2(H134R)-EYFP (Stanford Gene Vector and Virus Core) was microinjected into either the right LHb (anterior–posterior, with respect to bregma (AP), −1.58 mm; medial–lateral (ML), 0.5 mm; dorsal–ventral (DV]), 2.65 mm) or the right LDT (AP, −5.0 mm; ML, 0.5 mm; DV, 3.0 mm). To target the BLA for chemogenetic inhibition, AAV-DJ expressing the inhibitory DREADD receptor hM4Di and a fluorescent marker (mCherry; AAV-DJ-hSyn-hM4D(Gi)-mCherry) was microinjected directly into the BLA (AP, –1.3 mm; ML, 3.1 mm; DV, 5.0 mm). The DREADD virus was generated from plasmids from Addgene (donated by B. Roth).

Optrode implantation.—Optical fibers were constructed in-house by attaching 200 μm optical fiber (with a 0.37 numerical aperture) to a 1.25 mm zirconia ferrule (with the fiber extended 2 mm beyond the ferrule). Fibers were attached with epoxy resin into the ferrules, cut, and polished. Optical fibers were stabilized to the skull with screws and dental cement. Dental cement was painted black to minimize light leakage. For M72 photostimulation, optrodes were 9 mm long and implanted above the right, lateral M72 glomerulus (AP, 4.0 mm; ML, 1.1 mm; DV 0.9 mm). For VTA stimulation, optrodes were 12 mm long and implanted above either the right medial VTA (AP, –3.3 mm; ML, 0.3 mm; DV, 4.1 mm) or right lateral VTA (AP, –3.3 mm; ML, 0.5 mm; DV, 4.2 mm) to target projections from the LHb or the LDT according to a previously described method[15].

Photostimulation.

M72 photostimulation (CS) + footshock (US). Pulses of light (473 nm, 100 ms, 4 Hz, 20 mW) were used to approximate the average natural inhalation duration of a single sniff (100 ms) and frequency of respiration in mice (3–5 Hz)[44–49]. The 10 s photostimulation co-terminated with a 1 s footshock (0.7 mA), and mice received 10 M72 photostimulation–footshock pairings during training (Supplementary Fig. 4).

M72 photostimulation (CS) + VTA photostimulation (US).—To photostimulate LHb or LDT axonal input to the VTA, 15 pulses of 5 ms light flashes were delivered at 30 Hz every 2 s (473 nm, 20 mW) throughout the 15 min training session during which M72 photostimulation occurred continuously (473 nm, 100 ms, 4 Hz, 20 mW) (Supplementary Fig. 5) according to a previously described method[15].

General behavioral procedures.

Odor preparation.—An M72-activating odorant (acetophenone; A10701, Sigma-Aldrich) and a non-M72-activating odorant ((*S*)-(+)-carvone; 124931, Sigma-Aldrich) were used. Odorants were diluted in mineral oil (40% concentration) and stored in light-shielded vials. Before use, odorant (50 μl) was placed on filter paper on an inverted Petri dish lid (60 mm × 15 mm) and covered by a perforated Petri dish and cage bedding (Supplementary Fig. 1a).

General experimental procedures and apparatus.—There were three phases to the experiments: pre-exposure (day 1); train (day 2); and test (day 3). Mice were pre-exposed and tested for preference in a custom-designed preference test chamber (white Plexiglas, 15 cm × 45 cm × 25 cm) that was divided into two equally sized compartments (Supplementary Fig. 1b). Pre-exposure was 20 min in length, while the test was 10 min and occurred 1 day following training (this did not vary between experiments). During the pre-exposure phase, each compartment contained a non-scented Petri dish. During the preference test, each compartment contained a scented Petri dish (acetophenone or (S)-(+)-carvone, location randomly determined). Mouse behavior throughout the test was monitored via overhead cameras. Fiji ImageJ was used to track mouse position, and a customized code in R (v.3.2.2) computed the distance moved and the percentage time spent in either compartment. During the test, mouse preference was calculated as follows: percentage $\text{time}_{\text{acetophenone}}$ − percentage $\text{time}_{\text{carvone}}$.

Training (pairing a real or artificial CS with a real or artificial US) took place in a distinct, stainless steel chamber (31 cm × 24 cm × 21 cm), with shock-grid floors (bars 3.2 mm in diameter, spaced 7.9 mm apart). The front, top, and back of the chamber were clear acrylic, and the two sides were modular aluminum (Med Associates). The CS and US events (both real and artificial) were delivered as outlined below.

Experiments using real CS (acetophenone) and real US (footshock).—Mice were pre-exposed as above. On day 2 (training), mice were placed in the training chamber scented with acetophenone (40% concentration, 50 μl volume, placed in tray at the bottom of the chamber), and 1 min later, 10 footshocks (1 s, 0.7 mA, 1 min apart) were delivered. After the final footshock, mice remained in the training chamber for 60 s before being returned to their home cage. On day 3 (test), mice were placed in the test chamber with Petri dishes containing either acetophenone or carvone located in each compartment (the location of which was counterbalanced).

Experiments using real CS (acetophenone) and real US (food).—During training, food-deprived mice (24 h) were placed in the testing chamber (with the central divider removed), and a Petri dish scented with acetophenone (50 μl volume) was placed in the center of the apparatus. Small pieces of rodent chow were sprinkled throughout the bedding covering the Petri dish. Following training, mice remained food-deprived and were tested for acetophenone versus carvone preference 24 h later (Supplementary Fig. 6a).

Experiments using artificial CS (M72 photostimulation).—For experiments involving an artificial CS, behavioral training took place 1 week after optrode implantation.

Mice were habituated to the experimenter connecting the optical fibers to the optrodes for 3 days before the behavior experiments.

Experiments using artificial US (input to VTA photostimulation).—For experiments involving an artificial CS paired with an artificial US, behavioral training took place 4 weeks after AAV microinjection and 1 week after optrode implantation. Mice were habituated to the experimenter connecting the optical fibers to the optrodes for 3 days before the behavior experiments. During training, inputs to the VTA from the LHb (to mimic an aversive US) or from the LDT (to mimic an appetitive US) were stimulated throughout the duration of the 15 min training session in combination with photostimulation of the M72 glomerulus (Supplementary Fig. 5).

Specific experimental details.

Experiment 1 (acetophenone (CS) paired with footshock (US)).—Five groups of mice were used in this experiment. On day 1, mice were pre-exposed to the testing apparatus. During training (day 2), the mice underwent one of the following procedures: the CS was paired with the US (CS + US group; $n = 15$); the CS was presented alone ($n = 8$); the US was presented alone ($n = 15$); the CS and US were presented in an unpaired fashion (US | CS; $n = 12$); or mice were training-naive ($n = 8$). For the unpaired condition, the US and CS were presented as described above but separated by 24 h. Acetophenone versus carvone preference was tested 1 day after training.

Experiment 2 (M72 photostimulation (CS) paired with foot shock (US)).—Three groups of mice were used in this experiment. On day 1, mice were pre-exposed to the testing apparatus. During training, the mice received CS + US ($n = 18$), CS only ($n = 8$), or US | CS ($n = 8$). For the unpaired condition, the US and CS were presented as described above but separated by 24 h. Acetophenone versus carvone preference was tested 1 day after training.

Experiment 3 (M72 photostimulation (CS) paired with LHb–medial VTA photostimulation (US)).—Two groups of mice were used in this experiment. On day 1, mice were pre-exposed to the testing apparatus. During training, mice received either CS + US ($n = 12$) or US | CS ($n = 8$). For the unpaired condition, the US and CS were presented as described above but separated by 24 h. Acetophenone versus carvone preference was tested 1 day after training.

Experiment 4a (acetophenone (CS) paired with food (US)).—During training, mice received CS + US ($n = 12$). Acetophenone versus carvone preference was tested 1 day after training.

Experiment 4b (M72 photostimulation (CS) paired with LDT-lateral VTA photostimulation (US)).—Two groups of mice were used in this experiment. On day 1, mice were pre-exposed to the testing apparatus. During training, mice received either CS + US ($n = 10$) or US | CS ($n = 10$). For the unpaired condition, the US and CS were presented as described above but separated by 24 h. Acetophenone versus carvone preference was tested 1 day after training.

Experiment 4c (acetophenone (CS) paired with VTA photostimulation (US) in the absence of ChR2 expression).—On day 1, mice (n = 12) were pre-exposed to the testing apparatus. During training, mice received CS (acetophenone) paired with US (VTA photostimulation) presentation. Acetophenone versus carvone preference was tested 1 day after training.

Experiment 5a (Fos induction after recall of a real memory).—During training, mice received either acetophenone paired with footshock (CS + US; n = 6) or acetophenone only (CS only; n = 6). Twenty-four hours later, mice were placed in a regular Nalgene, mouse housing cage (without bedding) for a 6-min test during which the odor CS (acetophenone) was presented. Ninety minutes later, mice were perfused and their brains were processed for immunohistochemistry.

Experiment 5b (Fos induction after recall of an artificial memory).—During training, mice received either M72 photostimulation paired with LHb–medial VTA photostimulation (CS + US; n = 7) or M72 photostimulation (CS only; n = 8). Twenty-four hours later, mice were placed in a regular Nalgene, mouse housing cage (without bedding) for a 6-min test during which mice received 5 presentations of the artificial CS (10 s photostimulation, spaced 1-min apart). Ninety minutes later, mice were perfused and their brains were processed for immunohistochemistry. In both Experiments 5a and 5b, we normalized c-Fos expression in CS + US and CS only groups to levels in training-naive mice (n = 11).

Experiment 6 (BLA silencing and expression of a real memory).—Two groups of mice were used in this experiment. During training, mice received acetophenone paired with footshock (as above). Twenty-four hours later, mice were tested as above except that 1 h before the test, mice received either a systemic injection of the DREADD agonist C21 (ref. [17]) (1 mg per kg, i.p.; Tocris) (n = 9) or vehicle (PBS; n = 11). In addition, two groups of mice not expressing hM4Di were trained and tested as above. Before testing, mice received either vehicle (n = 12) or C21 (n = 12).

Experiment 7 (BLA silencing and expression of an artificial memory).—Two groups of mice were used in this experiment, which was designed similar to Experiment 6. During training, mice received M72 photostimulation paired with LHb–medial VTA photostimulation (as described above). Twenty-four hours later, mice were tested as above except that 1 h before the test, mice received either a systemic injection of the DREADD agonist C21 (1 mg per kg, i.p.; n = 7) or vehicle (n = 7).

Experiment 8 (in vivo assessment of chemogenetic inhibition).—To verify that C21 inhibits the activity of neurons expressing hM4Di, we microinjected AAV-DJ-hSyn-HA-hM4D(Gi)-mCherry bilaterally into the BLA of mice. Four weeks later, mice were trained and tested as described above (Experiments 6 and 7), and perfused 90-min later. Brains were collected and processed for c-Fos immunohistochemistry[50]. In these analyses, sample sizes were n = 3–4.

Immunohistochemistry.

Sagittal brain slices (50 μm) were incubated with blocking solution (0.1% BSA, 2% normal goat serum (NGS), 0.3% Triton X-100) for 1 h at room temperature. To visualize AAV-ChR2 labeled projections (Figs. 2c,h and 4h), sections were incubated with primary antibodies raised against tyrosine hydroxylase (TH; chicken, 1:1,000, Aves Labs) for 48 h at 4 °C. Sections were washed, incubated with Alexa Fluor 568 goat anti-chicken secondary antibody (1:500, Invitrogen) for 24 h at 4 °C.

To visualize c-Fos expression following recall of either real or artificial memories (Fig. 3; Supplementary Fig. 8), sections were incubated with a primary antibody raised against c-Fos (rabbit, 1:500; SC-52, Santa Cruz Biotechnology) for 48 h at 4 °C. Sections were washed, incubated with Alexa 568 or 633 goat anti-rabbit secondary antibody (1:500, Invitrogen) for 24 h at 4 °C.

Sections were washed, mounted on slides and coverslipped using PermaFluor mounting medium. Nuclei were counterstained with 4,6-diamidino-2-phenylindole (DAPI; Vectashield, Vector Labs). Images were obtained using a confocal laser scanning microscope (LSM 710, Zeiss).

To analyze c-Fos-positive nuclei in the network of brain regions (Experiments 5a and 5b), entire brain sagittal sections were acquired at ×20 magnification using the tile scan function. Analysis of c-Fos-positive nuclei was performed using the software Imaris (Bitplane). The borders of regions were defined manually according to the Franklin and Paxinos mouse brain atlas[51]. See Fig. 3c for sections acquired and regions selected. All imaging and analyses were performed blind to the experimental conditions.

To visualize projections, sections were acquired using the tile scan function, and filtered images were digitally combined to produce composite images using the software Photoshop.

To assess chemogenetic inhibition of the BLA region (Experiment 8), virally infected neurons were detected at lower magnification (×2 objective), then images were acquired at higher magnification (×20 objective, 5 *z*-stacks of 1 mm each). Equal cut-off thresholds were applied to all captures to remove background autofluorescence. AAV-hM4D-mCherry-positive cells co-stained with c-Fos were quantified using the software Image J (National Institute of Health).

iDISCO+ clearing and immunolabeling.

Dissected intact olfactory bulbs and the rostral portion of the forebrain were immunolabeled and cleared using an iDISCO+ protocol[52,53]. iDISCO+ included methanol dehydration, bleaching overnight in 5% hydrogen peroxide in methanol solution, and rehydration. Samples were then permeabilized (2 days at 37 °C with shaking) and placed in blocking solution (1× PBS with 0.2% Tween-20 and 10 mg ml^{-1} heparin (PTwH) mixed with 10% dimethylsulfoxide (DMSO) and 6% NGS) for 2 days at 37 °C with shaking. Samples were incubated in the primary antibody solution (PTwH with 5% DMSO and 3% NGS) with anti-green fluorescent protein (chicken, 1:2,000; 1020, Aves Lab) for 3 days at 37 °C with shaking. Samples were washed five times with PTwH for 1 h each, with the final wash

performed overnight. Samples were incubated in secondary antibody solution (PTwH with 3% NGS) and anti-chicken Alexa Fluor 633 (goat, 1:2,000; A-21103, Thermo Fisher) for 3 days at 37 °C with shaking, followed by washes (five times with PTwH, the final wash performed overnight, which included Sytox Orange (1:2,000; S34861, Thermo Fisher)). Clearing consisted of methanol dehydration with samples left overnight in 100% methanol, then incubated for 3 h in 66% dichloromethane (DCM; 270997, Sigma) and 33% methanol. Samples were washed twice in 100% DCM for 15 min and then placed in 100% dibenzyl ether (108014, Sigma).

Light sheet imaging and image processing.

Sample images were acquired on a light sheet microscope (Ultramicroscope I, LaVision BioTec) using a custom threedimensional (3D) printed base and optical adhesive (Norland Products, Optical Adhesive 61). Imaging parameters were as follows: a 4μm *z*-step size, 2.6 μm inplane resolution, 400 ms exposure using multichannel acquisition for 568 and 633 excitation wavelengths (60% laser power). Images were stitched using the software Fiji imaging[54]. The 3D projections were rendered using Imaris ×64 (Bitplane, v9.0.2) with a gamma correction for visualization purposes used for Sytox Orange.

Statistical analyses and reproducibility.

We evaluated both normality (Kolmogorov–Smirnov test) and homogeneity of variance (Bartlett or Brown–Forsythe test) for all datasets. For datasets that were normally distributed and had equivalent variance, parametric analysis of variance (ANOVA) or two-tailed *t*-tests (for independent samples) were used to assess group differences in behavior (for example, preference and distance moved) or histology (for example, *Fos* induction). Newman–Keuls post-hoc tests were used to directly assess group differences following ANOVA where appropriate. One sample *t*-tests (two-tailed) were used to assess whether mice expressed conditioned aversion or attraction (contrast versus no preference; that is, percentage $\text{time}_{\text{acetophenone}}$ − percentage $\text{time}_{\text{carvone}} = 0$). For datasets for which one or more of these assumptions was violated, we used a nonparametric Kruskal–Wallis ANOVA, followed by planned comparisons using Mann–Whitney *U*-tests. Pearson's correlations were used to assess linear relationships between variables (for example, CS-induced *Fos* expression in real versus artificial memory groups). Data were analyzed using GraphPad Prism (GraphPad Software).

In all experiments, mice were randomly assigned to different experimental conditions. In behavioral experiments, the experimenter was not blinded to the training condition. For the *Fos* analyses, the analyses were performed blind to the experimental condition. In behavioral experiments, multiple cohorts of experimental and control mice were used and yielded equivalent results. Pooled data from all cohorts were analyzed and are shown. Only mice that satisfied a priori histological criteria (correct optrode placement, and viral infection limited to the target region) were included in analyses. No statistical methods were used to predetermine sample sizes, but our sample sizes were similar to those reported in previous publications[12].

Reporting summary.

Further information on research design is available in the Nature Research Reporting Summary linked to this article.

Data availability

All data supporting the findings of this study are available from the corresponding author upon request.

code availability

Custom code for behavioral analysis is available from the corresponding author upon request.

Supplementary Material

Refer to Web version on PubMed Central for supplementary material.

Acknowledgements

This work was supported by Canadian Institute of Health Research (CIHR) grants to P.W.F. (FDN143227) and S.A.J. (MOP74650) and by National Institute of Mental Health grants to K.J.R. (R01-MH108665) and F.G.M. (F31-MH105237). S.A.J. is a CIHR Canada Research Chair in Memory Function and Dysfunction. P.W.F. is a CIHR Canada Research Chair in Cognitive Neurobiology. The authors thank A. Ramsaran and J. Johansen for comments on an earlier draft of this manuscript.

References

1. Eichenbaum H Still searching for the engram. Learn. Behav. 44, 209–222 (2016). [PubMed: 26944423]
2. Josselyn SA, Kohler S & Frankland PW Finding the engram. Nat. Rev. Neurosci. 16, 521–534 (2015). [PubMed: 26289572]
3. Tonegawa S, Liu X, Ramirez S & Redondo R Memory engram cells have come of age. Neuron 87, 918–931 (2015). [PubMed: 26335640]
4. Martin SJ & Morris RG New life in an old idea: the synaptic plasticity and memory hypothesis revisited. Hippocampus 12, 609–636 (2002). [PubMed: 12440577]
5. Buck L & Axel R A novel multigene family may encode odorant receptors: a molecular basis for odor recognition. Cell 65, 175–187 (1991). [PubMed: 1840504]
6. Buck LB The molecular architecture of odor and pheromone sensing in mammals. Cell 100, 611–618 (2000). [PubMed: 10761927]
7. Firestein S How the olfactory system makes sense of scents. Nature 413, 211–218 (2001). [PubMed: 11557990]
8. Mombaerts P et al. Visualizing an olfactory sensory map. Cell 87, 675–686 (1996). [PubMed: 8929536]
9. Ressler KJ, Sullivan SL & Buck LB Information coding in the olfactory system: evidence for a stereotyped and highly organized epitope map in the olfactory bulb. Cell 79, 1245–1255 (1994). [PubMed: 7528109]
10. Wang F, Nemes A, Mendelsohn M &Axel R Odorant receptors govern the formation of a precise topographic map. Cell 93, 47–60 (1998). [PubMed: 9546391]
11. Jones SV, Choi DC, Davis M & Ressler KJ Learning-dependent structural plasticity in the adult olfactory pathway. J. Neurosci. 28, 13106–13111 (2008).

12. Morrison FG, Dias BG & Ressler KJ Extinction reverses olfactory fear-conditioned increases in neuron number and glomerular size. Proc. Natl Acad. Sci. USA 112, 12846–12851 (2015).
13. Jiang Y et al. Molecular profiling of activated olfactory neurons identifies odorant receptors for odors in vivo. Nat. Neurosci. 18, 1446–1454 (2015). [PubMed: 26322927]
14. Smear M, Resulaj A, Zhang J, Bozza T & Rinberg D Multiple perceptible signals from a single olfactory glomerulus. Nat. Neurosci. 16, 1687–1691 (2013). [PubMed: 24056698]
15. Lammel S et al. Input-specific control of reward and aversion in the ventral tegmental area. Nature 491, 212–217 (2012). [PubMed: 23064228]
16. Cousens G & Otto T Both pre- and posttraining excitotoxic lesions of the basolateral amygdala abolish the expression of olfactory and contextual fear conditioning. Behav. Neurosci. 112, 1092–1103 (1998). [PubMed: 9829787]
17. Thompson KJ et al. DREADD agonist 21 (C21) is an effective agonist for muscarinic based DREADDs in vitro and in vivo. ACS Pharmacol. Transl Sci. 1, 61–72 (2018). [PubMed: 30868140]
18. Walker DL, Paschall GY & Davis M Glutamate receptor antagonist infusions into the basolateral and medial amygdala reveal differential contributions to olfactory vs. context fear conditioning and expression. Learn. Mem. 12, 120–129 (2005). [PubMed: 15774945]
19. Cowansage KK et al. Direct reactivation of a coherent neocortical memory of context. Neuron 84, 432–441 (2014). [PubMed: 25308330]
20. Gore F et al. Neural representations of unconditioned stimuli in basolateral amygdala mediate innate and learned responses. Cell 162, 134–145 (2015). [PubMed: 26140594]
21. Liu X et al. Optogenetic stimulation of a hippocampal engram activates fear memory recall. Nature 484, 381–385 (2012). [PubMed: 22441246]
22. Yiu AP et al. Neurons are recruited to a memory trace based on relative neuronal excitability immediately before training. Neuron 83, 722–735 (2014). [PubMed: 25102562]
23. Denny CA et al. Hippocampal memory traces are differentially modulated by experience, time, and adult neurogenesis. Neuron 83, 189–201 (2014). [PubMed: 24991962]
24. Tanaka KZ et al. Cortical representations are reinstated by the hippocampus during memory retrieval. Neuron 84, 347–354 (2014). [PubMed: 25308331]
25. Rashid AJ et al. Competition between engrams influences fear memory formation and recall. Science 353, 383–387 (2016). [PubMed: 27463673]
26. Ramirez S et al. Creating a false memory in the hippocampus. Science 341, 387–391 (2013). [PubMed: 23888038]
27. Redondo RL et al. Bidirectional switch of the valence associated with a hippocampal contextual memory engram. Nature 513, 426–430 (2014). [PubMed: 25162525]
28. Ohkawa N et al. Artificial association of pre-stored information to generate a qualitatively new memory. Cell Rep. 11, 261–269 (2015). [PubMed: 25843716]
29. Dudai Y in Science of Memory: Concepts (eds Roediger HL III, Dudai Y & Fitzpatrick SM) 13–16 (Oxford Univ. Press, 2007).
30. Shinkman PG, Swain RA & Thompson RF Classical conditioning with electrical stimulation of cerebellum as both conditioned and unconditioned stimulus. Behav. Neurosci. 110, 914–921 (1996). [PubMed: 8918995]
31. Steinmetz JE, Lavond DG & Thompson RF Classical conditioning in rabbits using pontine nucleus stimulation as a conditioned stimulus and inferior olive stimulation as an unconditioned stimulus. Synapse 3, 225–233 (1989). [PubMed: 2718098]
32. Hegoburu C, Parrot S, Ferreira G & Mouly AM Differential involvement of amygdala and cortical NMDA receptors activation upon encoding in odor fear memory. Learn. Mem. 21, 651–655 (2014). [PubMed: 25403452]
33. Sevelinges Y, Gervais R, Messaoudi B, Granjon L & Mouly AM Olfactory fear conditioning induces field potential potentiation in rat olfactory cortex and amygdala. Learn. Mem. 11, 761–769 (2004). [PubMed: 15537739]
34. McGann JP Associative learning and sensory neuroplasticity: how does it happen and what is it good for? Learn. Mem. 22, 567–576 (2015). [PubMed: 26472647]

35. Herry C & Johansen JP Encoding of fear learning and memory in distributed neuronal circuits. Nat. Neurosci. 17, 1644–1654 (2014). [PubMed: 25413091]
36. Ozawa T et al. A feedback neural circuit for calibrating aversive memory strength. Nat. Neurosci.20, 90–97 (2017). [PubMed: 27842071]
37. Di Scala G, Mana MJ, Jacobs WJ & Phillips AG Evidence of Pavlovian conditioned fear following electrical stimulation of the periaqueductal grey in the rat. Physiol. Behav. 40, 55–63 (1987). [PubMed: 3615655]
38. Kim EJ et al. Dorsal periaqueductal gray–amygdala pathway conveys both innate and learned fear responses in rats. Proc. Natl Acad. Sci USA 110, 14795–14800 (2013). [PubMed: 23959880]
39. Han S, Soleiman MT, Soden ME, Zweifel LS & Palmiter RD Elucidating an affective pain circuit that creates a threat memory. Cell 162, 363–374 (2015). [PubMed: 26186190]
40. Sato M et al. The lateral parabrachial nucleus is actively involved in the acquisition of fear memory in mice. Mol. Brain 8, 22 (2015). [PubMed: 25888401]
41. Tang J et al. Pavlovian fear memory induced by activation in the anterior cingulate cortex. Mol. Pain 1, 6 (2005). [PubMed: 15813993]
42. Johansen JP & Fields HL Glutamatergic activation of anterior cingulate cortex produces an aversive teaching signal. Nat. Neurosci. 7, 398–403 (2004). [PubMed: 15004562]
43. Tye KM & Deisseroth K Optogenetic investigation of neural circuits underlying brain disease in animal models. Nat. Rev. Neurosci. 13, 251–266 (2012). [PubMed: 22430017]

References

44. Carey RM & Wachowiak M Effect of sniffing on the temporal structure of mitral/tufted cell output from the olfactory bulb. J. Neurosci. 31, 10615–10626 (2011).
45. Doucette W et al. Associative cortex features in the first olfactory brain relay station. Neuron 69, 1176–1187 (2011). [PubMed: 21435561]
46. Rojas-Libano D & Kay LM Interplay between sniffing and odorant sorptive properties in the rat. J. Neurosci. 32, 15577–15589 (2012).
47. Shusterman R, Smear MC, Koulakov AA & Rinberg D Precise olfactory responses tile the sniff cycle. Nat. Neurosci. 14, 1039–1044 (2011). [PubMed: 21765422]
48. Wesson DW, Donahou TN, Johnson MO & Wachowiak M Sniffing behavior of mice during performance in odor-guided tasks. Chem. Senses 33, 581–596 (2008). [PubMed: 18534995]
49. Kepecs A, Uchida N & Mainen ZF The sniff as a unit of olfactory processing. Chem. Senses 31, 167–179 (2006). [PubMed: 16339265]
50. Vetere G et al. Chemogenetic interrogation of a brain-wide fear memory network in mice. Neuron 94, 363–374 (2017). [PubMed: 28426969]
51. Paxinos G & Franklin KBJ The Mouse Brain in Stereotaxic Coordinates (Academic Press, 2012).
52. Renier N et al. Mapping of brain activity by automated volume analysis of immediate early genes. Cell 165, 1789–1802 (2016). [PubMed: 27238021]
53. Renier N et al. iDISCO: a simple, rapid method to immunolabel large tissue samples for volume imaging. Cell 159, 896–910 (2014). [PubMed: 25417164]
54. Preibisch S, Saalfeld S & Tomancak P Globally optimal stitching of tiled 3D microscopic image acquisitions. Bioinformatics 25, 1463–1465 (2009). [PubMed: 19346324]

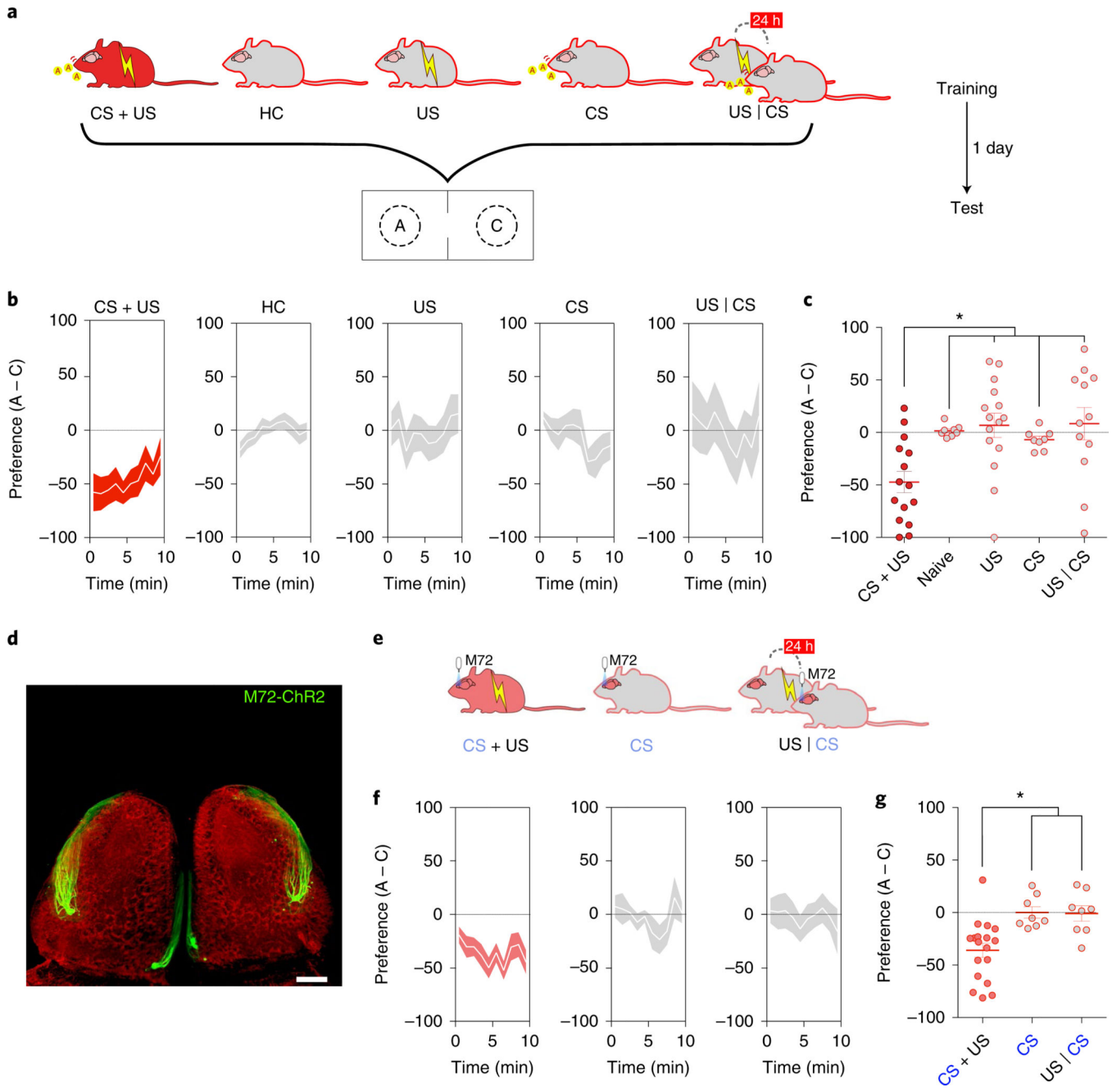

Fig. 1|. Pairing either acetophenone or M72 photostimulation with footshock produces conditioned odor aversion.

a, Mice were presented with different combinations of an odor CS (acetophenone) and a US (footshock) during training and tested 24 h later in a neutral apparatus containing the CS (acetophenone (A)) at one end and a distinct odor (carvone (C)) at the other (CS + US group, $n = 15$ mice; home cage (HC), $n = 8$ mice; US only, $n = 15$ mice; CS only, $n = 8$ mice; US | CS group, $n = 12$ mice). **b**, In a 10-min test, only conditioned mice (CS + US) avoided acetophenone (two-tailed, one sample t-test versus zero preference: CS + US group, $t_{14} = 4.66$, $P = 0.004$). The shaded region represents s.e.m. for the CS + US group (red) and

control groups (gray). **c**, Summary data showing that conditioned mice differed from each control group (unequal variance, Kruskal–Wallis, $\chi^2(4) = 15.73$, $P = 0.0034$; *Mann–Whitney U planned comparisons: CS + US versus HC, $U = 16$, $P = 0.0032$; CS + US versus US only, $U = 39.5$, $P = 0.0017$; CS + US versus CS only, $U = 23$, $P = 0.0159$, CS + US versus US | CS, $U = 36$, $P = 0.0074$). Error bars represent s.e.m. **d**, M72 glomeruli expressing ChR2-YFP (green) in the olfactory bulb of M72 mice. Scale bar, 500 μm. **e**, Mice were presented with different combinations of M72 photostimulation (CS; blue denotes artificial) and footshock (US) during training and tested 24 h later in a neutral apparatus containing acetophenone and carvone (CS + US group, $n = 18$ mice; CS only, $n = 8$ mice; US | CS group, $n = 8$ mice). **f**, In this test, only conditioned mice (CS + US) avoided acetophenone (two-tailed, one sample t-test versus zero preference: $t_{17} = 5.31$, $P < 0.0001$). The shaded region represents s.e.m. for the CS + US group (pink) and control groups (gray). **g**, Summary data showing that conditioned mice differed from each control group (ANOVA, $F_{2,31} = 8.91$, $P = 0.0009$, post hoc *$P < 0.05$). Error bars represent s.e.m.

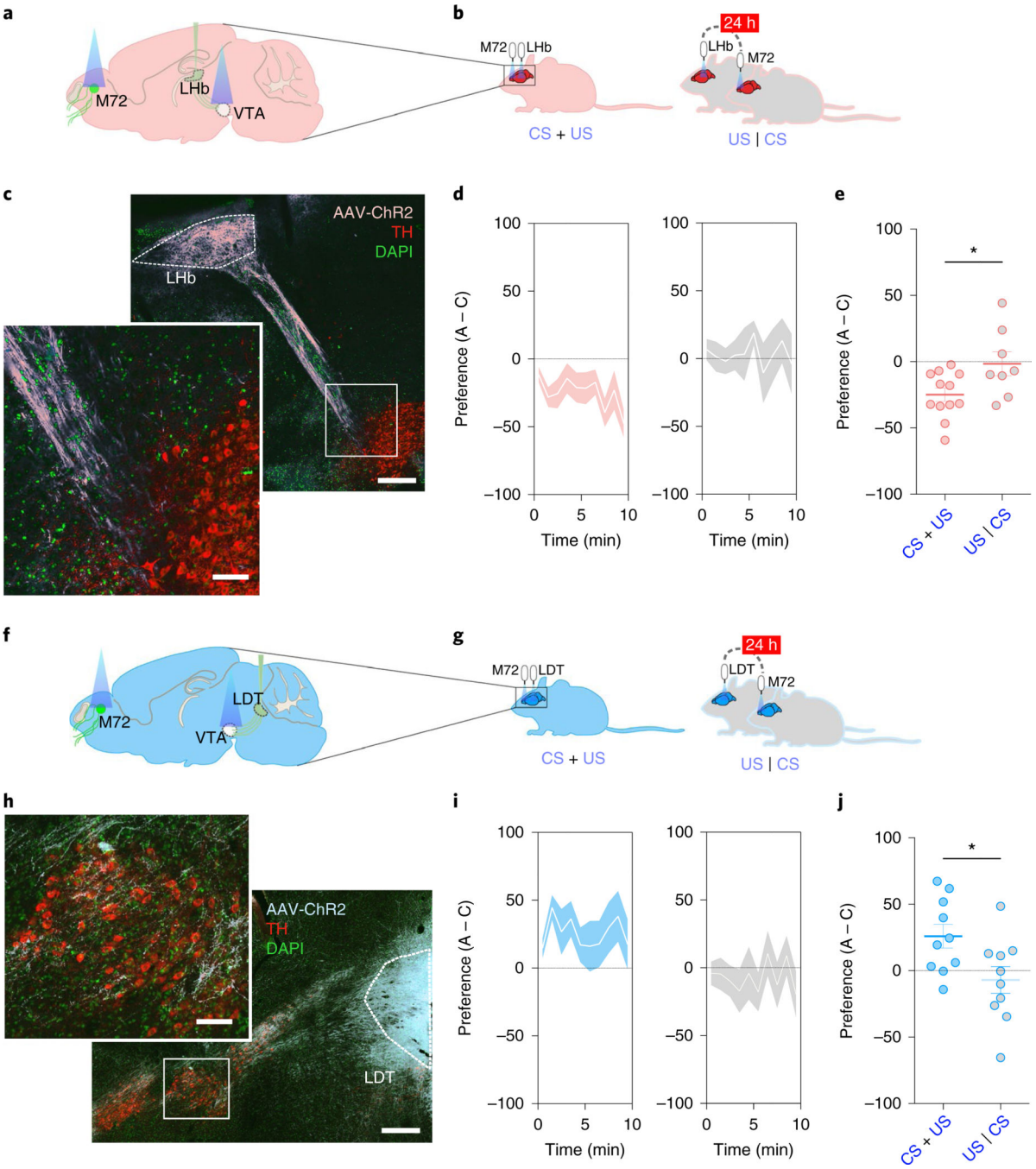

Fig. 2|. Generation of artificial memories by pairing M72 photostimulation with photostimulation of distinct LHb inputs into the VTA.

a,**b**, During training, M72 OSN afferent photostimulation was explicitly paired (CS + US, *n* = 12 mice) or not (US | CS, *n* = 8 mice) with photostimulation of the LHb terminal field in the medial VTA, and preference for M72-activating odorant (acetophenone) versus non-M72-activating odorant (carvone) was tested 24 h later. **c**, Low- and high-magnification (inset) images showing labeled LHb–VTA projections (pink) following infection of LHb with AAV-ChR2. Scale bars, 400 μm (low magnification), 100 μm (high magnification). **d**,

In the test, only conditioned mice (CS + US) avoided acetophenone (two-tailed, one sample *t*-test versus zero preference: $t_{11} = 4.96$, $P = 0.0004$). The shaded region represents s.e.m. for the CS + US group (pink) and US | CS group (gray). **e**, Summary data showing that preference in conditioned mice differed from that in control mice. CS and US shown in blue denote that these stimuli were artificial (two-tailed *t*-test: $t_{18} = 2.67$, $^{*}P = 0.016$). Error bars represent s.e.m. **f**,**g**, During training, M72 photostimulation was explicitly paired (CS + US, $n = 10$ mice) or not (US | CS, $n = 10$ mice) with photostimulation of the LDT terminal field in the lateral VTA, and preference for M72 odorant (acetophenone) versus non-M72 odorant (carvone) was tested 24 h later. **h**, Low- and high-magnification (inset) images showing labeled LDT–VTA projections (sky blue) following infection of LDT with AAV-ChR2. Scale bars, 400 μm (low magnification), 100 μm (high magnification). **i**, In the test, only conditioned mice (CS + US) were attracted to acetophenone (two-tailed *t*-test versus zero preference: $t_9 = 2.92$, $P = 0.017$). The shaded region represents s.e.m. for the CS + US group (blue) and US | CS group (gray). **j**, Summary data showing that preference in conditioned mice differed from that in control mice. CS and US shown in blue to denote that these stimuli were artificial (two-tailed *t*-test: $t_{18} = 2.45$, $^{*}P = 0.025$). Error bars represent s.e.m.

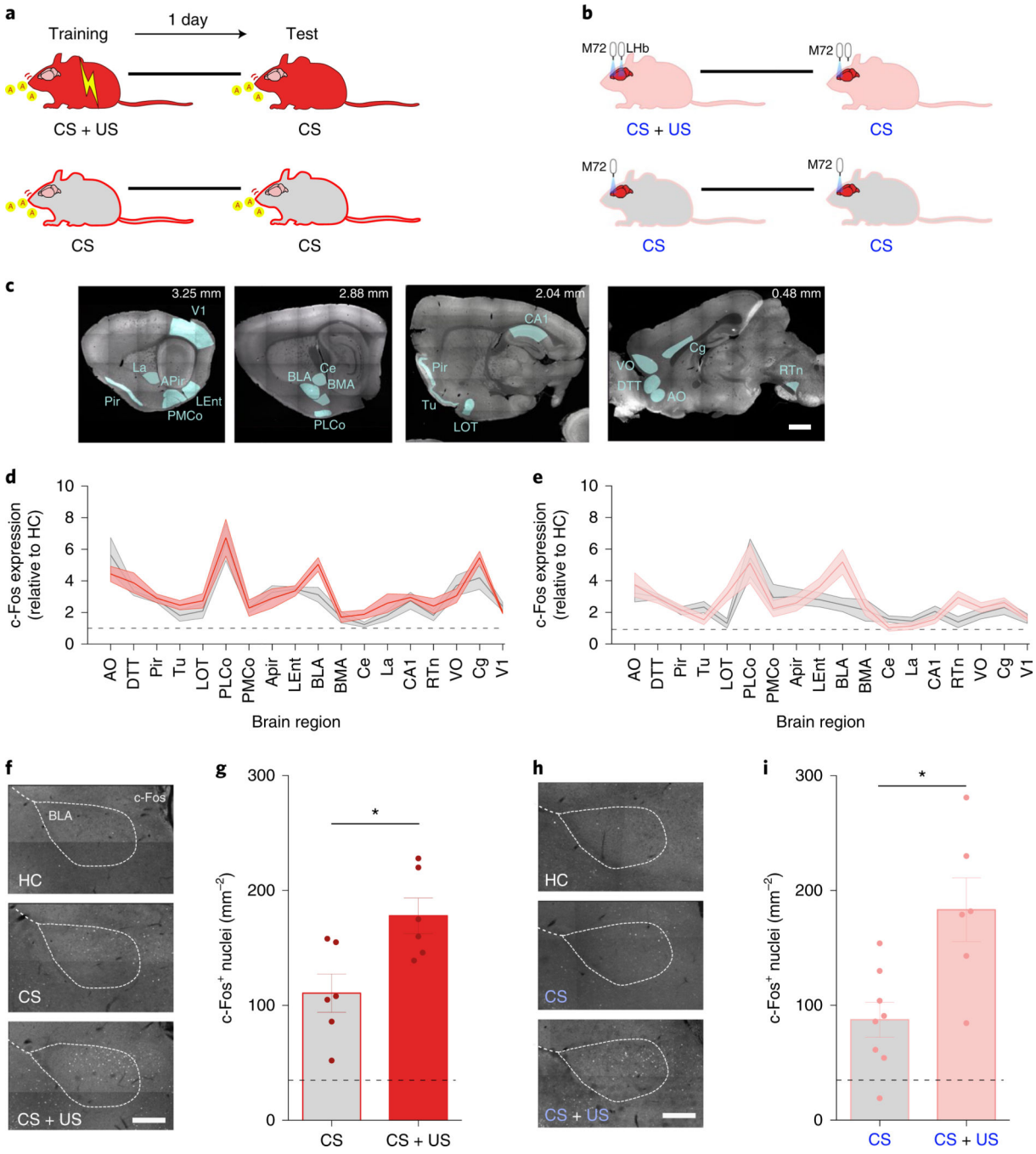

Fig. 3|. Real and artificial memories engage similar neural circuits.

a,**b**, In the real memory condition, during training mice were presented with either acetophenone alone (CS only, $n = 6$ mice) or acetophenone paired with footshock (CS + US, $n = 6$ mice). In the artificial memory condition, during training mice received either M72 photostimulation alone (CS only, $n = 8$ mice) or M72 photostimulation paired with photostimulation of LHb–VTA projections (CS + US, $n = 7$ mice). **c**, One day later, CS-induced *Fos* induction was analyzed in the central olfactory system and in regions involved in associative memory. These are sagittal sections, and numbers indicate distance from

midline. Scale bar, 1 mm. **d**,**e**, Fold changes in c-Fos expression in CS + US versus CS-only groups in the real (left) and artificial (right) memory conditions compared to training-naive control mice (broken black line). The shaded area represents s.e.m. **f**,**g**, Sagittal sections showing *Fos* induction (white) in the HC, CS and CS + US conditions. Scale bar, 100 μm. *Fos* induction was elevated in the BLA in mice that formed a real memory (two-tailed *t*-test: CS + US > CS only, $t_{10} = 2.97$, $^{*}P = 0.014$). **h**,**i**, Sagittal sections showing *Fos* induction (white) in the HC, CS and CS + US conditions. Scale bar, 100 μm. *Fos* induction was elevated in the BLA in mice that formed an artificial memory (two-tailed *t*-test: CS + US > CS only, $t_{12} = 3.24$, $^{*}P = 0.0071$). Broken black lines represent c-Fos expression levels in training-naive control mice. Error bars represent s.e.m. AO, anterior olfactory nucleus; DTT, dorsal tenia tecta; Pir, piriform cortex; Tu,olfactory tubercle; LOT, nucleus of the lateral olfactory tract; PLCo, osterolateral cortical amygdaloid nucleus; PMCo, posteromedial cortical amygdaloid nucleus; APir, amygdalopiriform transition area; LEnt, lateral entorhinal cortex; BMA, basomedial amygdaloid nucleus; Ce, central amygdaloid nucleus; La, lateral amygdaloid nucleus; CA1, field CA1 of the hippocampus; RTn, rostromedial tegmental nucleus; VO, ventral orbital cortex; Cg, cingulate cortex; V1, primary visual cortex.

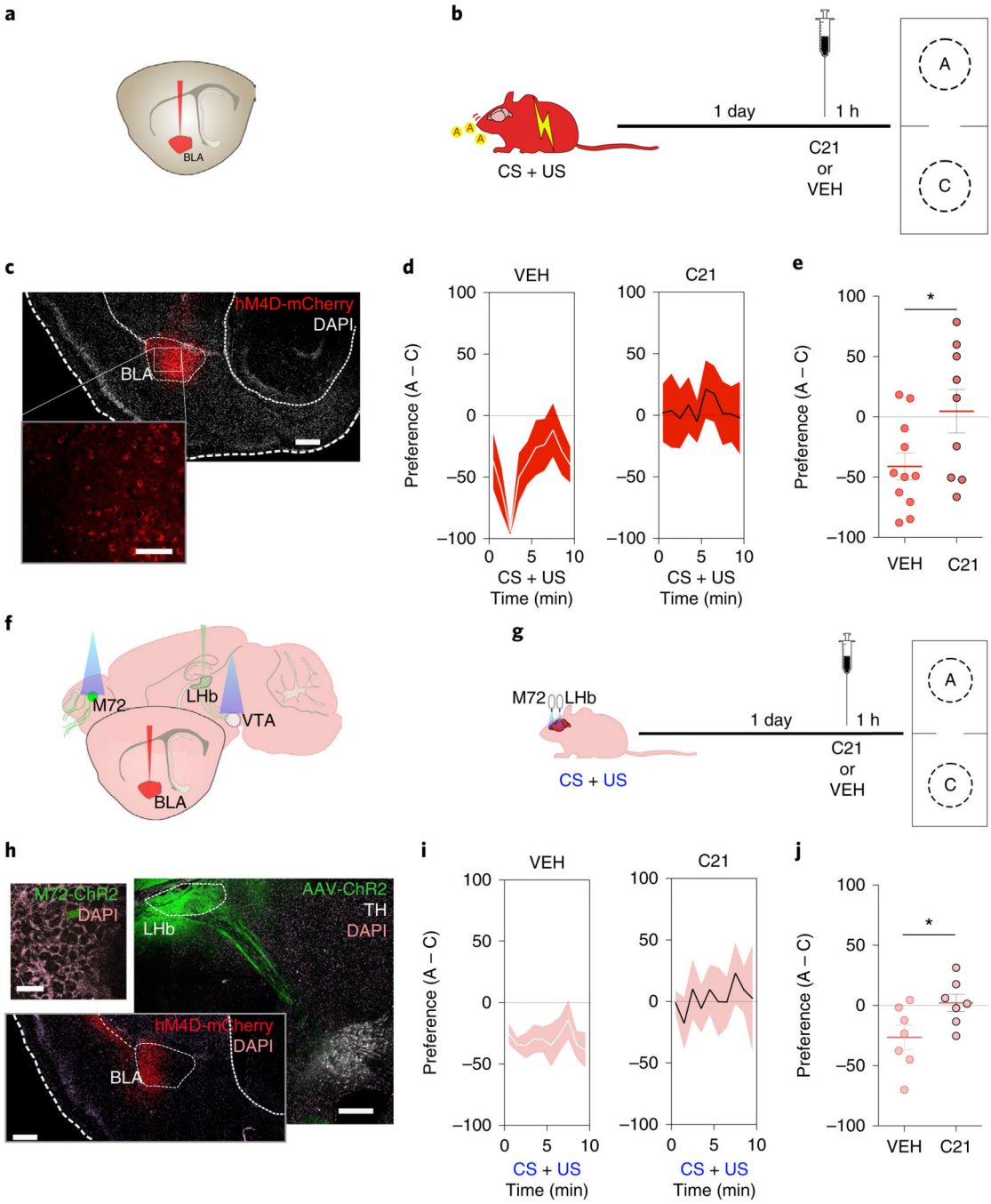

Fig. 4|. Silencing the BLA prevents expression of real and artificial odor memories.

a,**c**, AAV-hM4Di-mCherry was injected into the BLA of WT mice. Broken lines indicate anatomical boundaries. Scale bars, 100 μm (high magnification) and 400 μm (low magnification). **b**, During training, acetophenone was paired with footshock. Before testing, mice were treated with vehicle (VEH; $n = 11$) or C21 ($n = 9$). **d**, Only vehicle-treated mice avoided acetophenone (two-tailed, one sample t-test versus zero preference: $t_{10} = 3.70$, $P < 0.0041$). The shaded regions represent s.e.m. **e**, Summary data showing that preference in vehicle-treated and C21-treated mice differed (two-tailed t-test: $t_{18} = 2.24$, $^{*}P = 0.038$).

Error bars represent s.e.m. **f**,**h**, M72-ChR2 mice received infusions of AAV-hM4Di-mCherry into the BLA and AAV-ChR2 into the LHb. Optrodes were implanted above the M72 glomerulus and VTA. Broken lines indicate anatomical boundaries. Scale bars, 200 μm (top left, olfactory bulb), 400 μm (top right, LHb) and 400 μm (bottom, BLA). **g**, During training, M72 photostimulation was paired with photostimulation of LHb–VTA projections. Before testing, mice were treated with vehicle ($n = 7$) or C21 ($n = 7$). **i**, Only vehicle-treated mice avoided acetophenone (two-tailed, one sample *t*-test versus zero preference: $t_6 = 2.76$, $P = 0.033$). The shaded region represents s.e.m. **j**, Summary data showing that preference in vehicle-treated and C21-treated mice differed (two-tailed *t*-test: $t_{12} = 2.42$, $^*P = 0.033$). Error bars represent s.e.m.